

Phosphorescence and Triplet-State Optically Detected Magnetic Resonance Studies of Acetylacetonates of the Ammonium and Some Group 2 Metal Ions

J. J. Sahbari, K. D. Bomben, and D. S. Tinti*

Contribution from the Department of Chemistry, University of California, Davis, California 95616. Received April 4, 1983

Abstract: The phosphorescence and triplet-state optically detected magnetic resonance (ODMR) spectra of NH_4^+ , Be^{2+} , Mg^{2+} , Zn^{2+} , Ca^{2+} , and Ba^{2+} complexes of acetylacetonate are reported in EPA glass and for the group 2 complexes as neat crystals. The phosphorescence origins, phosphorescence lifetimes, and fine structure splittings of the $\pi\pi^*$ triplet state localized on the acetylacetonate anion are dependent on the cation. The results are compared to earlier studies of group 1 metal acetylacetonates and show a correlation to the cation radius that extends over the ammonium and group 1 and 2 metal complexes. An electrostatic perturbation of the acetylacetonate anion by the cation seems able to explain the observed variations in the triplet-state properties.

The perturbation of molecular electronic states by chemical substituents or solvents has been extensively studied. The related crystal-field interactions experienced by a metal cation are also well-known. However, the experimental observation of perturbations in the electronic states of anions due to interaction with cations is not so well documented. This reflects both the small number of anions whose electronic states have been studied in detail and the emphasis in metal complexes on d-d and charge-transfer transitions rather than ligand-localized transitions.

Acetylacetonate complexes of closed-shell metal ions provide a series wherein the perturbations experienced by the acetylacetonate anion due to interaction with cations can be systematically examined. The low-lying electronic states in these complexes are ligand localized with the triplet state phosphorescent at low temperatures.¹⁻⁴ We have initiated a detailed examination of the properties of the acetylacetonate triplet state, aimed at exposing and systematizing the perturbations caused by cations.⁵ The initial study dealt with alkali metal acetylacetonates and showed that the phosphorescence origins, phosphorescence lifetimes, and triplet-state fine structure splittings were correlated and sensitive to the alkali metal cation. The results in the alkali metal acetylacetonates were consistent with a simple electrostatic perturbation of the acetylacetonate (acac) anion by the alkali metal cation.

The present work was undertaken to check the correctness of our earlier interpretation of the trends in the group 1 complexes by extending the study to acetylacetonate complexes of the ammonium cation, a pseudo group 1 ion, and of various group 2 (Be^{2+} , Mg^{2+} , Zn^{2+} , Ca^{2+} , and Ba^{2+}) metal cations. The phosphorescence and triplet-state optically detected magnetic resonance (ODMR) spectra of the complexes at zero field and the triplet-state kinetic parameters have been obtained and analyzed. The results are similar to those reported earlier in the alkali metal complexes and show a correlation among the phosphorescence origins, triplet-state fine structure splittings, and cation size that extends over both the group 1 and 2 acetylacetonate complexes.

Experimental Section

Ammonium acetylacetonate was prepared by direct reaction between dry ammonia gas and freshly distilled acetylacetone at 0 °C. The resulting solid product is unstable at room temperature, liberating ammonia gas, but it can be stored without apparent decomposition at reduced temperatures. It is readily soluble in polar solvents, wherein it also

undergoes slow decomposition. The Raman spectrum at 77 K of the neat solid and the ¹H NMR spectrum at room temperature in CDCl_3 indicate that the complex is $\text{NH}_4(\text{acac})$.

The bis complexes of the group 2 metals were either obtained from commercial sources [$\text{Be}(\text{acac})_2$ and $\text{Zn}(\text{acac})_2 \cdot \text{H}_2\text{O}$; Alfa Products] or synthesized following the general method of Chalmers and Umar.⁶ The complexes were purified by recrystallization except for $\text{Be}(\text{acac})_2$, which was zone refined.⁷ Analysis of the complexes employed potentiometric titration of the acetylacetonate anion, volumetric or atomic absorption analysis for the metal cation, and/or X-ray diffraction methods.

$\text{Zn}(\text{acac})_2 \cdot \text{H}_2\text{O}$ was purified by multiple recrystallization from ethanol solution. Anhydrous $\text{Zn}(\text{acac})_2$ was prepared by multiple vacuum sublimation of the hydrated crystals at 80–90 °C.⁸ The Mg^{2+} and Ca^{2+} complexes were recrystallized from aqueous or water/methanol solutions. The crystal structures of the final products were determined by X-ray methods and the molecular formulas established as $\text{Mg}(\text{acac})_2 \cdot 2\text{H}_2\text{O}$ ⁹ and $\text{Ca}(\text{acac})_2 \cdot 3\text{H}_2\text{O}$.¹⁰ The corresponding anhydrous complexes were prepared by heating the hydrated crystals at ~140 °C under vacuum, followed by a rapid single recrystallization from anhydrous methanol. The Ba^{2+} complex was also recrystallized from methanol; analysis indicated that the crystalline complex was $\text{Ba}(\text{acac})_2$ and not hydrated.

A Ca^{2+} acetylacetonate complex was also prepared by mixing aqueous solutions of $\text{NH}_4(\text{acac})$ and a stoichiometric excess of calcium acetate. A crystalline product precipitated slowly (overnight) from the solution. A determination of its crystal structure showed that the complex contained acetylacetonate and acetate (OAc) with a molecular formula $\text{Ca}(\text{acac})(\text{OAc}) \cdot 2\text{H}_2\text{O}$. The crystal contains chains of $[\text{Ca}(\text{acac}) \cdot 2\text{H}_2\text{O}]^+$ moieties symmetrically bridged by acetate ions. Any datum that refers to this complex will be explicitly noted. No attempt was made to purify this complex after its preparation.

The optical and triplet-state ODMR spectra were obtained for the various complexes as neat crystals and as $\sim 5 \times 10^{-4}$ M solutions in EPA (ethanol:isopentane:ethyl ether 2:5:5) by using previously described instrumentation.⁵ The hydrated and anhydrous complexes of Mg^{2+} , Zn^{2+} , and Ca^{2+} gave identical results in EPA insofar as they were checked. However, since the hydrated complexes were generally more readily dissolved in EPA, and thus judged less likely to precipitate as microcrystals in forming the glass, the results quoted in EPA refer to the hydrated complexes as solutes.

Results

The phosphorescence emission and photoexcitation spectra of acetylacetonate complexes of the ammonium ion and group 2 metal ions in EPA glass at 77 K are very similar to those reported earlier for the group 1 metal complexes,⁵ namely, the somewhat structured phosphorescence spectrum has its origin at ~390 nm and its photoexcitation maximum appears at ~305 nm. Figure

(1) Crosby, G. A.; Watts, R. J.; Westlake, S. J. *J. Chem. Phys.* **1971**, *55*, 4664.

(2) Ohno, T.; Kato, S. *Bull. Chem. Soc. Jpn.* **1974**, *47*, 1901.

(3) Clarke, R. H.; Connors, R. E. *Spectrochim. Acta, Part A* **1974**, *30*, 2063.

(4) Kemlo, J. A.; Neilson, J. D.; Shepherd, T. M. *J. Inorg. Nucl. Chem.* **1977**, *39*, 1945. Kemlo, J. A.; Shepherd, T. M. *J. Chem. Soc., Faraday Trans.* **1977**, *73*, 1850.

(5) Sahbari, J. J.; Tinti, D. S. *Mol. Phys.* **1983**, *48*, 419.

(6) Chalmers, R. A.; Umar, M. *Anal. Chim. Acta* **1968**, *42*, 357.

(7) Isao, Y.; Hiroshi, K.; Keihei, U. *Talanta* **1977**, *24*, 58.

(8) Bennett, M. J.; Cotton, F. A.; Eiss, R. *Acta Crystallogr., Sect. B* **1968**, *24*, 904.

(9) Morosin, B. *Acta Crystallogr.* **1967**, *22*, 315.

(10) Sahbari, J. J.; Olmstead, M. M. *Acta Crystallogr., Sect. C* **1983**, *39*, 208.

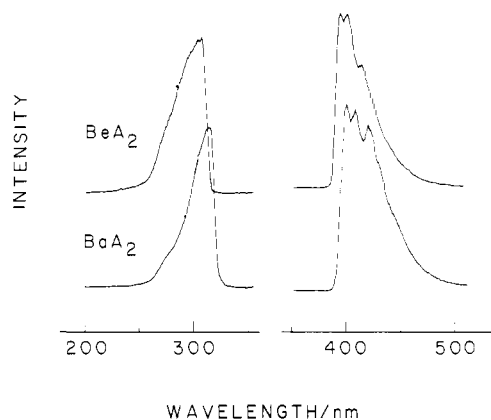


Figure 1. Phosphorescence emission and photoexcitation spectra of $\text{Be}(\text{acac})_2$ and $\text{Ba}(\text{acac})_2$ in EPA at 77 K.

Table I. Properties of the Triplet State of the Acetylacetonate Complex of the Ammonium and Group 2 Metal Ions in EPA

cation	origin/ nm	life- time/ ms ^a	$\tau_i -$ τ_z / GHz ^b	k_i / s ⁻¹ c	k_z / s ⁻¹ c	D / cm ⁻¹ d	E / cm ⁻¹ e
NH ₄ ⁺	403	195	2.38	1.22	19.2	0.127	0.040
			2.62	0.88			
Be ²⁺	391.0	104	2.05	1.20	29.4	0.130	0.062
			3.72	1.04			
Mg ²⁺	391.5	306	2.11	0.71	10.5	0.128	0.057
			3.44	0.54			
Zn ²⁺	391.5	285	2.18	0.77	11.8	0.131	0.058
			3.49	0.68			
Ca ²⁺	393.8	265	2.12	0.76	11.6	0.127	0.056
			3.38	0.62			
Ba ²⁺	400.0	50	2.87	3.29	66.7	0.136	0.041
			2.43	1.03			

^a At 4.2 K; ± 5 ms. ^b ± 0.03 GHz. ^c $\pm 10\%$. ^d $D \equiv -3X/2$.
^e $E \equiv (Y - Z)2$.

1 compares the spectra of $\text{Be}(\text{acac})_2$ and $\text{Ba}(\text{acac})_2$, which represent the two extremes in spectral position among the investigated acetylacetonate complexes of group 2 metals. Table I gives the phosphorescence origins in EPA for the complexes studied in this work. When the ammonium ion is considered as a "pseudo" group 1 ion and the data are compared to the earlier data,⁵ the phosphorescence origins show a monotonic shift to longer wavelengths with increasing cation size within a group and from group 1 to group 2 for cations of similar size. These trends are shown in Figure 2.

The phosphorescence lifetimes, included in Table I for the complexes studied in this work and shown in Figure 2 for all of the group 1 and 2 complexes, do not show such clear trends. A limited trend exists among the group 1 metal complexes, but the lifetime for the pseudo group 1 complex $\text{NH}_4(\text{acac})$ seems somewhat too long. Among the group 2 complexes any trend is less evident. However, if the lifetime of the most covalent complex, $\text{Be}(\text{acac})_2$, is discounted, the phosphorescence lifetimes of the remaining complexes roughly shorten with increasing cation size.

The ODMR derived results for the complexes of the ammonium and the group 2 metal ions in EPA at 1.4 K are also summarized in Table I. The results again are very similar to those reported earlier for the complexes of group 1 metal ions. Two broad ODMR signals, both corresponding to a phosphorescence intensity increase, were seen in each complex in the range 2–4 GHz. With various ODMR techniques,¹¹ the total phosphorescence rates k_i and estimates of the relative radiative rates k_i^r associated with each spin level τ_i ($i = x, y, z$) of the phosphorescent triplet state were determined. The rates k_i are given in Table I with the unique rate adjacent to the corresponding ODMR frequency. The

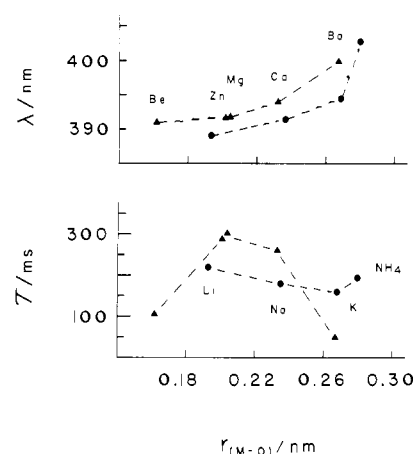


Figure 2. Variation of the phosphorescence origin and lifetime of group 1 (●) and 2 (▲) metal acetylacetonates in EPA at 4.2 K with metal-oxygen distance.

common rate, called k_z , is listed in a separate column. The results show that $k_z \gg k_x \approx k_y$ and that k_z is ~ 3 times the phosphorescence rate at ≥ 4 K. The radiative rates, not listed in Table I, were also found to order $k_z^r \gg k_x^r \approx k_y^r$ with $k_z^r/k_i^r \geq 10$.

On the basis of the similarities of the optical and ODMR results between the complexes with group 1 and 2 metal ions, the assignments in the bis complexes of the group 2 ions are made neglecting any resonance interaction between the acetylacetonate ions and, therefore, extrapolated from the experimental and calculational results reported earlier.⁵ Accordingly, the emitting triplet state is taken as localized in one acetylacetonate moiety having ideal C_{2v} symmetry with the z -axis parallel to the C_2 symmetry axis, the x -axis normal to the plane of the anion, neglecting the methyl hydrogens, and the y -axis in the plane and orthogonal to the x - and z -axes. The lowest energy triplet state in the acetylacetonate ion becomes 3B_2 ($\pi_4^* \leftarrow \pi_3$), from which τ_z is expected to be most radiative, and in which the calculated absolute order of the spin levels is $\tau_y > \tau_z > \tau_x$.⁵

However, as in the group 1 complexes, an ambiguity exists in assigning the two observed ODMR frequencies to the $\tau_y - \tau_z$ and $\tau_z - \tau_x$ transitions and, therefore, in the fine structure constants. We present the latter in Table I only for the particular choice that was concluded to be more probable in the alkali metal complexes.⁵ Namely, we assume that in the more covalent complexes (smaller cations) the frequencies of the ODMR transitions have $\tau_y - \tau_z > \tau_z - \tau_x$. In terms of the usual fine structure constants, this choice has $Y > 0$ and $X < Z < 0$ or $D \equiv -3X/2 > 0$ and $E \equiv (Y - Z)/2 > 0$ with $D < 3E$. With this assignment, the ODMR signal intensities order $I(\tau_z - \tau_x) > I(\tau_y - \tau_z)$ and the phosphorescence rates order $k_z > k_x > k_y$ for the more covalent complexes with group 2 metal ions. We assume that the relative signal intensities and the ordering of the phosphorescence rates are maintained in the more ionic complex with Ba^{2+} so that the ODMR frequencies now have $\tau_y - \tau_z < \tau_z - \tau_x$ ($Y > Z > 0$ and $X < 0$). The choice for $\text{NH}_4(\text{acac})$ is similarly extrapolated from the alkali metal complexes (by maintaining $k_z > k_y > k_x$) and also leads to $Y > Z > 0$ and $X < 0$. The above correlations, based on maintaining the ordering of the phosphorescence rates and the relative ODMR signal intensities in the complexes with metal ions from the same group, necessitate a change in the sign of Z with increasing size of the cation. Namely, among the group 1 complexes, $Z < 0$ for Li^+ and Na^+ , $Z \approx 0$ for K^+ , and $Z \geq 0$ for NH_4^+ ; among the group 2 complexes, $Z < 0$ for Be^{2+} , Mg^{2+} , Zn^{2+} , and Ca^{2+} and $Z > 0$ for Ba^{2+} . The trends are shown in Figure 3 where the parameters D and E are graphed vs. the corresponding metal-oxygen distance in the complex, taken from crystal structure determinations^{8-10,12-16}

(12) Stewart, J. M.; Morosin, B. *Acta Crystallogr., Sect. B* **1975**, *31*, 1164.

(13) Montgomery, H.; Lingafelter, E. C. *Acta Crystallogr.* **1963**, *16*, 748.

(14) Schröder, F. A.; Weber, H. D. *Acta Crystallogr., Sect. B* **1975**, *31*,

1745. Onuma, S.; Shibata, S. *Rep. Fac. Sci. Shizuoka Univ.* **1978**, *12*, 45.

(15) Sahbari, J. J.; Olmstead, M. M. *Acta Crystallogr., Sect. C*, in press.

(11) Tinti, D. S.; El-Sayed, M. A. *J. Chem. Phys.* **1971**, *54*, 2529. Winscom, C. J.; Maki, A. H. *Chem. Phys. Lett.* **1971**, *12*, 264. Schmidt, J.; Antheunis, D. A.; van der Waals, J. H. *Mol. Phys.* **1971**, *22*, 1.

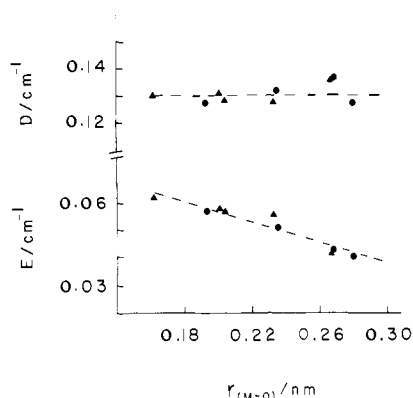


Figure 3. Variation of the fine-structure splitting parameters in the triplet state of group 1 (●) and 2 (▲) metal acetylacetonates in EPA at 1.4 K with metal-oxygen distance.

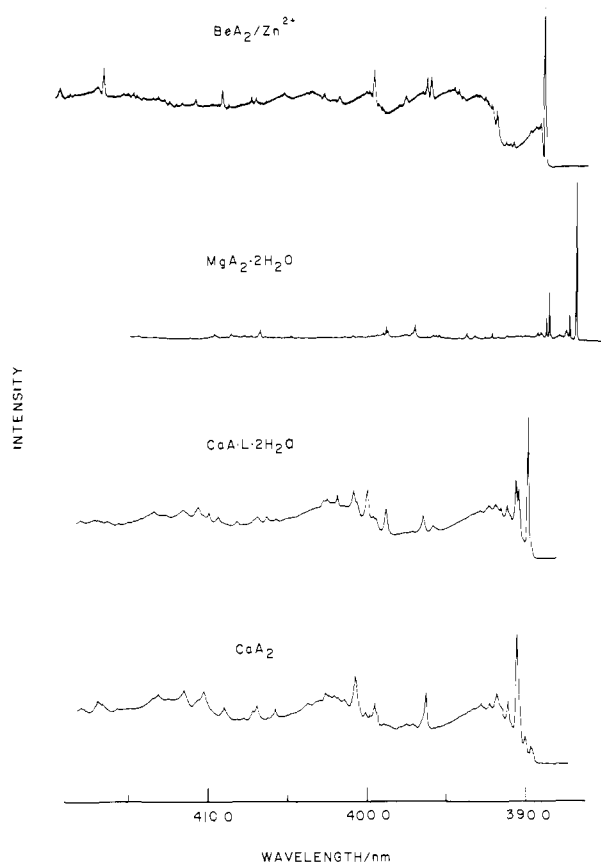


Figure 4. Phosphorescence emission spectra of some neat group 2 metal acetylacetonates at 1.4 K. CaA·L·2H₂O represents Ca(acac)(OAc)·2H₂O.

or estimated from tables of ionic radii.¹⁷ The results show that in the complexes with group 1 or 2 metal ions D is relatively constant, but E is strongly variable, decreasing with increasing metal-oxygen distance. If the alternate choice is made for the more covalent complexes but the correlations within a group are again made by maintaining the ordering of the phosphorescence rates and the relative ODMR signal intensities, D remains roughly constant but E increases with increasing cation size. The group correlations are perhaps questionable in the K⁺, NH₄⁺, and Ba²⁺ complexes. However, since $|Z| \ll |X| \approx |Y|$ in these cases, the deduced values of D and E are not significantly changed by the reverse assignments for the observed ODMR resonances. In

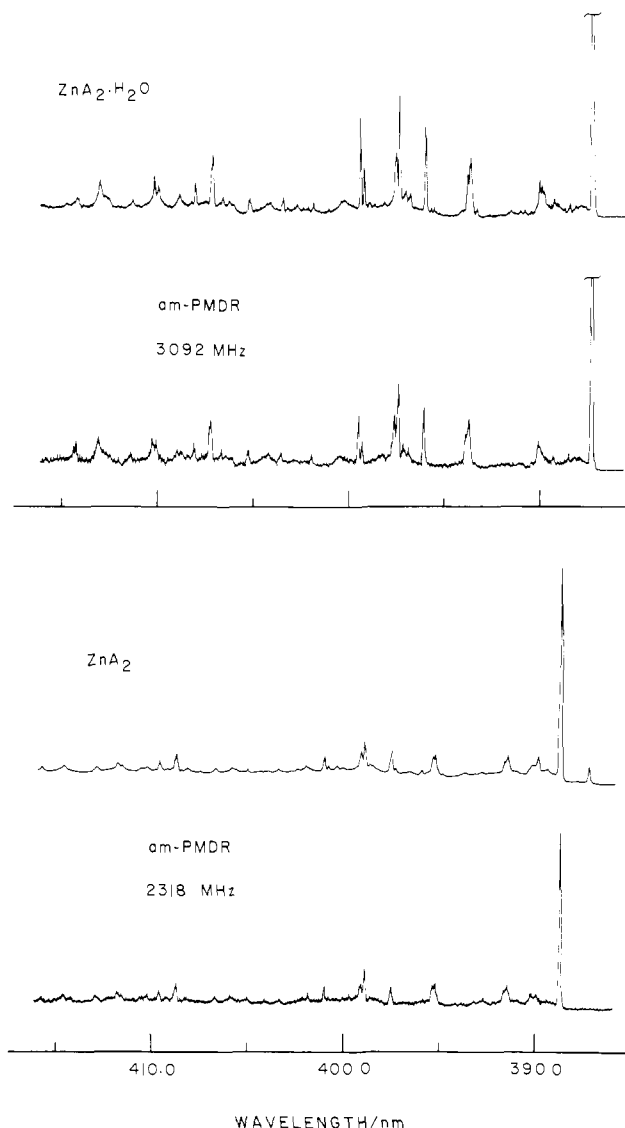


Figure 5. Comparison of the phosphorescence emission and am-PMDR spectra of neat Zn(acac)₂ and Zn(acac)₂·H₂O at 1.4 K. The resonant microwave frequency for each am-PMDR spectrum is indicated.

particular, D remains roughly constant while E is strongly dependent on the size of the cation.

Similar data were also obtained for neat polycrystals of the group 2 metal acetylacetonates at ≤ 4 K. The bis complexes of Mg²⁺, Zn²⁺, and Ca²⁺ were studied as hydrated and anhydrous crystals; the Ca²⁺ complex was studied in addition as Ca(acac)(OAc)·2H₂O; the Be²⁺ and Ba²⁺ bis complexes were studied only as anhydrous crystals. All of the neat crystals showed moderately intense and structured phosphorescence, presumably from "traps", based on origins at 380–400 nm. Representative spectra are shown in Figures 4 and 5.

The spectra of Mg²⁺ and Zn²⁺ complexes are dominated by one trap in either the hydrated or anhydrous crystals with the origin of the dominant trap in the hydrated crystal blue-shifted from that in the anhydrous crystal by 130 and 100 cm⁻¹, respectively. Aside from the shifts in the origins, the spectra of the Mg²⁺ and Zn²⁺ complexes are all very similar. The three Ca²⁺ complexes showed characteristically different phosphorescence spectra. The relatively weak phosphorescence of neat Ca(acac)₂·3H₂O appears dominated by one trap at 389.68 nm, but at higher resolution the apparent single origin resolves into three lines of comparable intensities with a total splitting of 13 cm⁻¹. The spectrum of anhydrous Ca(acac)₂ is based on a major trap at 390.58 nm, red-shifted from that in the hydrated crystal by 59 cm⁻¹. The spectrum of Ca(acac)(OAc)·2H₂O has its origin at 389.85 nm. The phosphorescence of neat Ba(acac)₂ is broad

(16) Shibata, S.; Onuma, S.; Matsui, Y.; Motezi, S. *Bull. Chem. Soc. Jpn.* **1975**, *48*, 2516.

(17) Huheey, J. E. "Inorganic Chemistry: Principles of Structure and Reactivity"; Harper and Row: New York, 1972; pp 74–75.

Table II. Vibronic Analysis of the Major Trap Phosphorescence in Neat $\text{Zn}(\text{acac})_2 \cdot \text{H}_2\text{O}$

$\lambda_{\text{air}}/\text{nm}$	rel ^a int	$\nu_{\text{vac}}/\text{cm}^{-1}$	$\Delta\nu/\text{cm}^{-1}$	assignment ^b
387.245	vs	25 816.1	0	
389.26	vw	25 682	134	
389.80	w	25 647	169	172 R, IR
389.92	w	25 639	177	
390.04	w	25 631	185	
393.32	vw	25 417	399	395 R
393.62	m	25 398	418	423 R, IR
393.82	m	25 385	431	434 R, IR
396.05	ms	25 242	574	573 R, IR
396.80	vw	25 194	622	
397.05	vw	25 179	637	
397.37	s	25 158	658	657 R, IR
397.57	m	25 146	670	670 R
399.23	m	25 042	774	772 IR
399.42	ms	25 029	786	779 IR, R
400.3	m,vb	24 973	843	$2 \times 418, 418 + 431, 2 \times 431$
401.87	vw	24 877	940	945 R, IR
402.72	vw	24 824	992	$418 + 574$
402.88	vw	24 814	1002	$431 + 574$
403.22	vw	24 793	1023	1022 R, IR
403.45	vw	24 780	1036	1037 R
404.01	vw	24 745	1071	$418 + 658$
404.27	vw	24 729	1087	$431 + 658, 418 + 670$
405.25	w	24 671	1145	2×574
406.07	vw	24 619	1197	$418 + 774, 574 + 622$
406.27	vw	24 607	1208	$418 + 786, 431 + 774, 574 + 637$
406.62	vw	24 586	1230	$431 + 786, 574 + 658$
406.77	vw	24 577	1239	$574 + 670$
407.12	m	24 556	1260	1264 R, IR
408.04	w	24 500	1316	$2 \times 658, 1310 \text{ R}$
408.64	vw	24 464	1352	$574 + 774, 418 + 940$
408.82	w,b	24 453	1363	$574 + 786, 431 + 940, 1360 \text{ R}$
409.97	w	24 385	1431	$658 + 774$
410.17	w	24 373	1443	$658 + 786, 670 + 774, 418 + 1023$
411.33	vw	24 305	1511	$574 + 940, 1515 \text{ R}$
413.04	w,b	24 204	1612	$670 + 940, 1616 \text{ R}$
414.24	vw,b	24 134	1682	$418 + 1260, 431 + 1260, 1675 \text{ R}$

^a s, strong; m, medium; w, weak; v, very; b, broad. ^b Based on our Raman (R) results and the infrared (IR) data of ref 18.

with only the origin at 399.2 nm resolved.

A vibronic analysis of the stronger lines associated with the major trap in $\text{Zn}(\text{acac})_2 \cdot \text{H}_2\text{O}$ is presented as an example in Table II. Although the analysis is tentative and perhaps hampered by the occurrence of zinc isotopes, the major vibronic intervals are readily correlated with the vibrational frequencies of neat $\text{Zn}(\text{acac})_2 \cdot \text{H}_2\text{O}$ obtained from our Raman results and reported infrared data.¹⁸ The vibronic analyses and the relative intensities for the stronger lines in crystals of the anhydrous Zn^{2+} complex, the anhydrous and hydrated Mg^{2+} and Ca^{2+} complexes, and in $\text{Ca}(\text{acac})(\text{OAc}) \cdot 2\text{H}_2\text{O}$ are similar. Table III compares the main fundamental vibrational frequencies of the neat hydrated crystals of the preceding bis complexes obtained from the vibronic analysis of their major trap phosphorescence at ≤ 4 K with Raman results at room temperature.

The neat-crystal phosphorescence spectra of most of the complexes are largely independent of sample with only minor variability seen. The latter appears due in large part to the degree of hydration. For example, the emission from polycrystalline samples of the Mg^{2+} or Zn^{2+} complexes can consist of both the hydrated and anhydrous traps. The further treatment of the samples generally increases the intensity of the appropriate trap, but only rarely is the other trap eliminated entirely.

However, the phosphorescence of neat $\text{Be}(\text{acac})_2$ is rather dependent on the sample and temperature with several traps

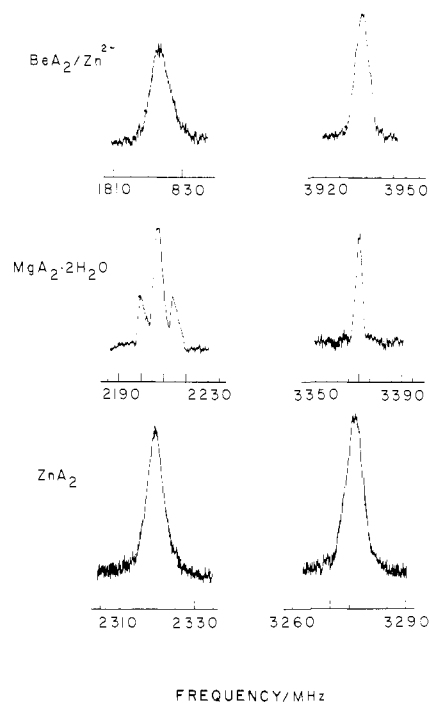


Figure 6. Example slow-passage ODMR spectra at 1.4 K for the triplet state of the major trap in neat group 2 metal acetylacetonates.

emitting with comparable intensities. It was not possible for us to obtain neat crystals that would consistently yield an emission spectrum dominated by one trap. We chose, therefore, to generate a trap by doping $\text{Be}(\text{acac})_2$ with low concentrations of $\text{Zn}(\text{acac})_2$ by cosublimation. The phosphorescence spectra of these doped crystals consistently show a sharp origin at 388.75 nm whose intensity increases with dopant concentration. Although emission from host traps at mainly lower energies was still present, and variable, certain vibronic intervals associated with the 388.75 nm origin could be determined. These are included in Table III, along with those from one of the host traps (origin at 392.07 nm). A phosphorescence spectrum of $\text{Be}(\text{acac})_2/\text{Zn}^{2+}$ is included in Figure 4.

The data in Table III indicate that the trap emissions from the neat crystals are associated with a host moiety, and not some impurity. This even seems to be the case for $\text{Be}(\text{acac})_2$ doped with $\text{Zn}(\text{acac})_2$. All spectra show a strong origin and only weak vibronic activity, involving mainly 400–800- cm^{-1} modes and a $\sim 1250\text{-cm}^{-1}$ mode. The frequencies and relative intensities of the active modes in the phosphorescence spectra are similar in all of the group 2 complexes and also similar to those in $\text{Na}(\text{acac}) \cdot \text{H}_2\text{O}$.⁵ This further indicates that the excited triplet state is localized on the acetylacetonate anion and that its geometry is similar in all of the complexes.

Two ODMR resonances were detected at 1.4 K by monitoring the origin of the major trap phosphorescence in each of the various crystalline complexes with group 2 metals except $\text{Ca}(\text{acac})_2 \cdot 3\text{H}_2\text{O}$, which was not studied by ODMR due to its weak phosphorescence intensity. The wavelengths (in air) of the monitored origins and the peak frequencies of the ODMR resonances are given in Table IV with example slow-passage ODMR spectra shown in Figure 6. The third ODMR resonance was detected in those systems searched by fast-passage methods at the sum of the frequencies given in Table IV. Some of the slow-passage signals (Mg^{2+} and undoped Be^{2+} complexes) exhibited resolved structure with power-dependent satellites at about ± 7 MHz from the strong center line. We assume this represents proton hyperfine interaction from the methyl groups of the acetylacetonate anion, but no attempt was made to analyze the splittings. The deduced phosphorescence rates k_i and relative radiative rates k_i^r for the crystalline systems are also given in Table IV.

The ODMR frequencies are similar and show the same general trends with metal ion for the traps in the neat crystals as for the

Table III. Fundamental Vibrations in cm^{-1} of Crystalline Bis(acetylacetonate) Complexes from Phosphorescence (P) and Raman (R) Spectra

$\text{Be}^{2+}/\text{Zn}^{2+}$	Be^{2+}		$\text{Mg}^{2+}\cdot 2\text{H}_2\text{O}$		$\text{Zn}^{2+}\cdot \text{H}_2\text{O}$		$\text{Ca}^{2+}\cdot 3\text{H}_2\text{O}$		$\text{Na}^+\cdot \text{H}_2\text{O}^a$	
	P	P	R	P	R	P	R	P	R	P
458	453	443	420	417	418	423	402	402	380	380
474	484	482	455	452	431	434				
563	563	568	564	570	574	573	575	572	582	580
			587							
658	662	662	662	660	658	657	648	650	645	643
673	669				670	670				
689	700	694								
		780	770	764	774	780	769	764	784	780
			778		786					
	1305	1301	1267	1262	1260	1264	1259	1259	1237	1235

^a Data from ref 5.

Table IV. Properties of the Triplet State of the Major Trap in Group 2 Metal Acetylacetonate Crystals

cation	origin/ nm	$(\tau_i - \tau_z)/\text{GHz}$	k_i/k_a	k_z/k_a	k_z^x/k_i^x	D/cm^{-1}	E/cm^{-1}
Be^{2+}	392.10	1.895	1.39	37.7		0.1280	0.0648
		3.892	1.87				
$\text{Be}^{2+}/\text{Zn}^{2+}$	388.75	1.824	1.61	13.2	8	0.1264	0.0656
		3.933	1.22		20		
Mg^{2+}	388.62	2.132	0.225	14.3	35	0.1290	0.0579
		3.475	0.45		25		
$\text{Mg}^{2+}\cdot 2\text{H}_2\text{O}$	386.67	2.207	0.21	18.5	80	0.1297	0.0562
		3.370	0.37		40		
Zn^{2+}	388.74	2.318	0.79	28.6	45	0.1319	0.0546
		3.276	1.5		36		
$\text{Zn}^{2+}\cdot \text{H}_2\text{O}$	387.25	2.439	0.88	31.2	40	0.1328	0.0515
		3.092	1.35		30		
Ca^{2+}	390.58	2.295	0.41	21.3	20	0.1268	0.0503
		3.02	1.0	>15			
$\text{Ca}^{2+}\cdot 2\text{H}_2\text{O}^d$	389.85	2.366	0.41	26.0	20	0.1295	0.0507
		3.04	0.83	>15			
Ba^{2+}	399.20	2.84	7.46	83.3	12	0.134	0.039
		2.36		>10			

^a $\pm 10\%$. ^b $\pm 20\%$. ^c $D \equiv -3X/2$. ^d $E \equiv (Y - Z)/2$.^e $\text{Ca}(\text{acac})(\text{OAc})\cdot 2\text{H}_2\text{O}$.

complexes in EPA. The fine structure constants $D \equiv -3X/2$ and $E \equiv (Y - Z)/2$ for the crystalline traps, also presented in Table IV, are based on the same assumptions outlined earlier. We note that the phosphorescence rates in the group 2 complexes have $k_z > k_y > k_x$ in the neat crystals whereas $k_z > k_x \geq k_y$ was observed in EPA. In the alkali metal complexes the same order for the phosphorescence rates was found in EPA and the neat crystals.⁵ However, the phosphorescence radiative activity originates from the middle electron-spin level τ_z in both the neat crystals and EPA ($k_z^x/k_i^x > 10$) for all of the complexes. The total and radiative phosphorescence rates are somewhat atypical for the doped system $\text{Be}(\text{acac})_2/\text{Zn}^{2+}$, but the ODMR frequencies are much closer to those in neat $\text{Be}(\text{acac})_2$ than in neat $\text{Zn}(\text{acac})_2$ or $\text{Zn}(\text{acac})_2\cdot \text{H}_2\text{O}$. Taken together with the vibrational frequencies of Table III, the total data for $\text{Be}(\text{acac})_2/\text{Zn}^{2+}$ show that the properties of the phosphorescent trap generated by doping are more like a perturbed $\text{Be}(\text{acac})_2$ host complex than the $\text{Zn}(\text{acac})_2$ guest, even allowing for a change to tetrahedral coordination in $\text{Zn}(\text{acac})_2$ as a guest from the nontetrahedral coordination in neat $\text{Zn}(\text{acac})_2^8$ or $\text{Zn}(\text{acac})_2\cdot 2\text{H}_2\text{O}^{13}$.

The emissions of neat $\text{Zn}(\text{acac})_2$ and $\text{Zn}(\text{acac})_2\cdot \text{H}_2\text{O}$ were further investigated by recording am-PMDR¹⁹ spectra at their stronger ODMR resonances, which were given in Table IV. One am-PMDR spectrum in each system is compared with the corresponding normal phosphorescence in Figure 5. The origin and all of the stronger vibronic lines in the phosphorescence of the major trap were detected in both am-PMDR spectra with the same sign and with similar relative intensities as in the normal phosphorescence spectrum. Hence, the stronger vibronic lines have

similar radiative phosphorescence rates as the origin and, thus, also originate principally from τ_z .

Discussion

The results obtained herein for the acetylacetonate complexes of the ammonium ion and the various group 2 metal ions largely parallel and extend the results found earlier in the corresponding complexes of the alkali metal ions. We focus on the results for the complexes in EPA where the solvent perturbations are presumably roughly constant, whereas for the traps in the crystalline systems the "solvent" perturbations are distinctly different. In EPA the properties of the triplet state of the complexes are sensitive to the cation with the phosphorescence origin, triplet-state fine structure splittings, and cation size clearly correlated, as shown in Figures 2 and 3, with the correlations extending over cations from both group 1 and group 2. Figure 2 shows that any trend in the total phosphorescence lifetimes, which parallel the behavior of k_z^{-1} , is considerably less clear, although the lifetimes for cations larger than Be^{2+} roughly shorten with increasing cation size. The results in the crystalline systems, particularly in the fine-structure splittings, support the trends and correlations found for the complexes in EPA.

The data indicate that the emitting triplet state is ligand localized in all of the complexes and in bis complexes of group 2 metals further localized on one acetylacetonate anion rather than delocalized over the two anions. In the latter case the tetrahedral complex $\text{Be}(\text{acac})_2$ would have $D \neq E = 0$, discounting Jahn-Teller distortion in the orbitally degenerate delocalized triplet state. Further, the variation in the fine structure splittings (for the crystal traps) in the nontetrahedral complexes are not explainable in terms of a dimer model using a constant D and E for the monomer acetylacetonate anion and the known angles^{8-10,13} between the axes of the two acetylacetonate anions in the neat group 2 complexes. The dimer model is also eliminated by the phosphorescence rates which show that τ_z remains the single active level in the phosphorescence origin for all of the complexes. Spin-orbit interactions centered on the cation can also be eliminated as a major contributor to the observed variations since the properties of the NH_4^+ and Zn^{2+} complexes correlate with their respective cation sizes. This is particularly evident comparing the Zn^{2+} and Mg^{2+} complexes, which have essentially the same triplet-state properties and cation radii, although the spin-orbit coupling on Zn^{2+} should be much larger.

Hence, the variations seen in the properties of the triplet state of the complexes appear due to perturbation of the local electronic structure of the acetylacetonate anion by an essentially electrostatic interaction with the cation. Since complexes of group 1 and 2 cations of similar size have similar triplet-state properties, the effective charge of the group 2 cations must be reduced in the complex to near unity as in the group 1 cations, presumably because of the second acetylacetonate (or acetate) anion. Thus, the simple electrostatic model presented earlier⁵ to explain the variations in the triplet-state properties of the alkali metal complexes should also be applicable to the complexes of the ammonium ion and the group 2 metal ions.

This model considered the acetylacetonate anion within the framework of Hückel theory and incorporated an electrostatic

(19) El-Sayed, M. A.; Owens, D. V.; Tinti, D. S. *Chem. Phys. Lett.* **1970**, *6*, 395.

interaction with a cation, located on the $z(C_2)$ -axis adjacent to the oxygen atoms, by relative adjustment of the oxygen Coulomb integral. As the distance along the z -axis between the acetylacetonate anion and the cation, or alternately the cation radius, increases, the oxygen Coulomb integral decreases. Accordingly, the properties of the ligand-localized ${}^3B_2(\pi_4^* \leftarrow \pi_3)$ state of the complex would vary smoothly with the cation radius for a constant effective charge on the cation.

In particular, the model predicts the phosphorescence origin to red-shift and the phosphorescence (radiative) lifetime to shorten as the cation radius increases.⁵ The experimental trends in the phosphorescence origins are in good agreement, with the additional red shift in the group 2 complexes implying a slightly decreased effective positive charge for the cation. The experimental phosphorescence lifetimes only qualitatively agree with the predicted trend, but we feel the agreement is satisfactory. The calculations considered perturbation of only the π -electronic structure in evaluating the relevant spin-orbit mixing term $\langle \pi_3 | \mathcal{H}_{SO}(z) | n \rangle \Delta E$. Changes in the n -electronic structure and energy denominator should also be important. Further, the calculations refer explicitly to k_z^r whereas the experimental results at best refer to $k_z = k_z^r + k_z^{nr}$. The lifetime in $Be(acac)_2$ is an obvious exception to even the qualitative trend, but its neglect is justified since it is the only definitively tetrahedral and the most covalent complex studied. The triplet state of a tetrahedral bis(acetylacetonate) complex correlates to 3E in D_{2d} symmetry, which is subject to Jahn-Teller distortion. In EPA or the neat crystal at low temperature, phosphorescence would originate from a distorted potential minimum having only C_{2v} symmetry. The interactions causing the distortion and localization of the excitation may well be manifest as a shortened phosphorescence lifetime, reflecting vibronic radiative and/or radiationless activity.

The fine-structure splittings of the 3B_2 state are also calculated to change within the model.⁵ If only the spin-spin contributions are considered, and approximated by the two-center Coulomb-type terms, $D \equiv -3X/2$ is calculated to decrease slightly and $E \equiv (Y - Z)/2$ to decrease significantly as the cation radius increases. The trends in the second-order spin-orbit contributions to D and E are more difficult to evaluate. The most important terms arise from interactions with the lowest excited singlet and triplet states of a different orbital character, namely the ${}^{1,3}B_1(\pi_4^* \leftarrow n)$ states. However, the variation of the relevant energy gaps with cation is not intuitively simple. Photoelectron spectra of $Be(acac)_2$ and $Zn(acac)_2$ give the $\pi_3(b_1) - n(b_2)$ orbital splitting as 1.3 and 0.8 eV, respectively.^{20,21} We interpret these as indicating that the ${}^{1,3}B_1(\pi_4^* \leftarrow n) - {}^3B_2(\pi_4^* \leftarrow \pi_3)$ energy gaps also decrease as the cation radius increases. Assuming that the spin-spin and spin-orbit contributions to the fine structure tensor have identical principal axes, the fine structure constants are simply the sum of the two contributions: $D = D_{SS} + D_{SO}$ and $E = E_{SS} + E_{SO}$. If the spin-orbit terms are limited to mixing with the ${}^{1,3}B_1$ states, then

$$D_{SO} = -E_{SO} = | \langle \mathcal{H}_{SO}(z) \rangle |^2 (\Delta E_{TT}^{-1} - \Delta E_{ST}^{-1})$$

where $\Delta E_{TT} = E({}^3B_1) - E({}^3B_2)$ and $\Delta E_{ST} = E({}^1B_1) - E({}^3B_2)$. Hence, D would increase and E decrease by the same amount due to the spin-orbit contributions as the cation radius increases. The two contributions thus lead to opposite changes in D with cation radius, but reinforce each other in causing E to decrease with increasing cation radius, in agreement with the experimental trends in the acetylacetonate complexes of both the group 1 and 2 cations.

Among all of the acetylacetonate complexes, the mean values of the fine-structure constants in EPA are $D = 0.131 \pm 0.004$ and $E = 0.052 \pm 0.008$ cm^{-1} . These compare with $D = 0.114$ and $E = 0.050$ cm^{-1} calculated for the two-center Coulomb-type spin-spin interactions in the 3B_2 state of the acetylacetonate anion perturbed by an effective charge of +1 on the z -axis at 0.20 nm

from the oxygen atoms.⁵ The agreement indicates that the spin-orbit contributions are not important in the magnitudes of the fine structure constants. The variation in D and E also cannot be attributed solely to changes in the spin-orbit mixing with ${}^{1,3}B_1$ states. If the latter were true, $D + E$ would remain constant at $D_{SS} + E_{SS}$ since $D_{SO} = -E_{SO}$. However, Figure 3 shows that the decrease in E occurs at approximately twice the slope as any increase in D , so that $D + E$ is not constant. Hence, the spin-spin contributions are also not constant, in agreement with the calculations.⁵ In summary, although the influence of the spin-orbit interactions in the variation of the fine-structure constants cannot be eliminated, the data seem to require changing spin-spin contributions.

We note, however, that the experimental zero-field splittings are sensitive to more than just the identity of the cation and thereby the metal-oxygen distance. This is demonstrated by the rather broad widths of the ODMR signals in EPA and by the results in the crystalline systems. Comparing either the main traps in the hydrated and anhydrous neat crystals with the same cation (Mg^{2+} or Zn^{2+}) or different traps in a neat crystal (Na^+ or Be^{2+}) shows the sensitivity of the fine structure splittings in acetylacetonate complexes to the details of the environment. Between the hydrated and anhydrous complexes of Mg^{2+} and Zn^{2+} the changes in the triplet-state properties are in the direction expected within the model since coordination of water to the metal ion should reduce its effective charge. However, energy shifts of the ${}^{1,3}B_1$ states relative to the 3B_2 state caused by different environments would change the spin-orbit interactions and could also be important.

The vibronic analyses of the phosphorescence spectra in the neat complexes are generally consistent with the elementary description of the 3B_2 state as arising from the $\pi_4^* \leftarrow \pi_3$ orbital excitation. Both the π_3 and π_4^* orbitals are antibonding across the C-O bonds, but the π_4^* orbital has in addition a nodal xz -plane (containing the C-H bond). Hence, the Franck-Condon activity in the phosphorescence spectrum is expected to emphasize modes that involve the C-CH-C grouping. This agrees with the infrared assignments¹⁸ of the modes active in the phosphorescence of neat $Zn(acac)_2 \cdot H_2O$: $\nu(C=C=C)$ at ~ 1260 cm^{-1} , $\gamma(C-C-H)$ at ~ 770 cm^{-1} , and ring deformations coupled with metal-oxygen stretches at ~ 650 , ~ 570 , and ~ 420 cm^{-1} . The trends shown in Table III indicate that the same assignments apply in the other complexes. The detailed symmetries of these modes may not be important to their activity, since in the low-symmetry crystalline field of the emitting trap all may correlate to totally symmetric modes. Hence, their activity need not represent vibronic mixings. The am-PMDR results in $Zn(acac)_2 \cdot H_2O$, which indicate that the corresponding vibronic bands originate predominantly from the same spin level (τ_2) as the electronic origin, support such an interpretation, although a_2 and b_1 modes could also be active in emission from 3B_2 τ_2 .

Summary

The properties of the ${}^3(\pi\pi^*)$ state of the acetylacetonate anion, particularly the fine structure splittings, are quite sensitive to the cation and correlate to the cation size for cations from groups 1 and 2. The observed trends are explainable in terms of a simple electrostatic interaction between an effective unit positive charge representing the cation and the acetylacetonate anion. The triplet states of other anions will clearly be similarly perturbed by closed-shell metal cations, although other more complicated interactions may also be manifest if the cation orbitals are not energetically distant from the anion orbitals. The latter can include, for example, spin-orbit mixing with charge-transfer states. Even greater perturbations of the triplet-state properties can then result due to large one-center spin-orbit terms on a heavy-metal cation. However, for the acetylacetonate complexes investigated in this work, such effects are not significant.

Kemlo and Shepherd⁴ have previously concluded that heavy-atom spin-orbit effects are unimportant in the phosphorescence lifetimes of diamagnetic metal acetylacetonates, except perhaps in the complexes of Th^{4+} , Lu^{3+} , and La^{3+} , and In^{3+} . They sug-

(20) Evans, S.; Hammett, A.; Orchard, A. F.; Lloyd, D. R. *Faraday Discuss. Chem. Soc.* **1972**, *54*, 227.

(21) Fragala, I.; Costanzo, L. L.; Ciliberto, E.; Condorelli, G.; D'Arrigo, C. *Inorg. Chim. Acta* **1980**, *40*, 15.

gested that the changes in the phosphorescence lifetimes were due to changes in the mixing between the $^3(n\pi^*)$ and $^3(\pi\pi^*)$ states caused by their changing energy differences. A smaller polarizing power (charge/radius ratio) for the metal ion would lead to a smaller energy difference and larger mixing between the $^3(n\pi^*)$ and $^3(\pi\pi^*)$ states, causing the lifetime of the triplet state to shorten because of increased $^3(n\pi^*)$ character. We find no need to involve nor evidence to support this explanation. The changes in the

phosphorescence lifetimes can result simply from changes in the spin-orbit mixing between the $^1(n\pi^*)$ and $^3(\pi\pi^*)$ states.

Acknowledgment. We thank M. M. Olmstead for providing analyses of some of the complexes by x-ray diffraction methods.

Registry No. $\text{NH}_4(\text{acac})$, 86392-33-8; $\text{Be}(\text{acac})_2$, 10210-64-7; $\text{Mg}(\text{acac})_2$, 14024-56-7; $\text{Zn}(\text{acac})_2$, 14024-63-6; $\text{Ca}(\text{acac})_2$, 17372-36-0; $\text{Ba}(\text{acac})_2$, 17372-35-9; $\text{Ca}(\text{acac})(\text{OAc})\cdot 2\text{H}_2\text{O}$, 86392-34-9.

Photochemistry of $\text{Ru}(\text{bpy})_3^{2+}$. Solvent Effects

Jonathan V. Caspar and Thomas J. Meyer*

Contribution from the Department of Chemistry, University of North Carolina, Chapel Hill, North Carolina 27514. Received July 23, 1982

Abstract: The excited-state lifetime of the metal-to-ligand charge-transfer (MLCT) excited state or states of $\text{Ru}(\text{bpy})_3^{2+}$ has been measured in a series of solvents at a series of temperatures. The data can be fit to the equation $\tau(T)^{-1} = k + k'^0 \exp[-(\Delta E'/k_B T)]$ where k is the sum of the radiative (k_r) and nonradiative (k_{nr}) rate constants for decay of the MLCT state(s) and the temperature-dependent term involves a thermally activated transition from the MLCT state to a low-lying state or states presumably d-d in character. From a combination of lifetime and emission quantum yield measurements, values for k_r and k_{nr} have been obtained in the series of solvents. From the variations of the various kinetic parameters with solvent the following conclusions can be reached: (1) k_r is only slightly solvent dependent; (2) the variations in k_{nr} and emission energy with solvent are in quantitative agreement with the predictions of the energy gap law for radiationless transitions; and (3) the solvent dependence of the kinetic parameters k'^0 and $\Delta E'$, which characterize the MLCT \rightarrow dd transition, can be considered in the context of electron-transfer theory including the observation of a linear relationship between $\ln k'^0$ and $\Delta E'$ (Barclay-Butter plot). In a final section the implications of solvent effects on the use of $\text{Ru}(\text{bpy})_3^{2+}$ as a sensitizer are discussed.

We have shown that the energy gap law can be applied to nonradiative decay in a series of polypyridyl complexes of Os(II).^{1,2} The studies were based on the metal-to-ligand charge-transfer (MLCT) excited states of the two series of complexes (phen)- $\text{Os}^{\text{II}}\text{L}_4^{2+}$ and $(\text{bpy})\text{OsL}_4^{2+}$ (bpy is 2,2'-bipyridine, phen is 1,10-phenanthroline; L = $1/2$ bpy, $1/2$ phen, pyridine, PR_3 , Me_2SO , CH_3CN , ...). The nature of the experiment was to show from excited-state lifetime and emission measurements that plots of $\ln k_{nr}$ vs. E_{em} are linear where k_{nr} is the nonradiative decay rate constant and E_{em} the emission energy. In addition, it was possible to account for the origin of the solvent dependence of k_{nr} on the basis of the energy gap law using the series of Os-phen based MLCT excited states.³ In these studies, radiative rate constants, k_r , for excited-state decay, were shown to be relatively insensitive to variations either in complex or in solvent.

The earlier studies based on the Os(II) complexes are part of a larger effort to explore in detail the photochemical and photophysical properties of MLCT excited states. In many ways the "parent" compound associated with MLCT excited states is $\text{Ru}(\text{bpy})_3^{2+}$. The excited-state electronic structures of $\text{Ru}(\text{bpy})_3^{2+}$ and related complexes have been investigated by spectroscopic studies,⁴ low-temperature emission and lifetime measurements,⁵

and theoretical studies.⁶ The excited state(s) of $\text{Ru}(\text{bpy})_3^{2+}$ has been frequently used in sensitization processes based on electron-transfer quenching.⁷

Because of its importance, it is desirable to establish in detail the photochemical and photophysical properties of $\text{Ru}(\text{bpy})_3^{2+}$. Compared to related complexes of Os(II), there is an additional complication for complexes of Ru(II) associated with the intervention of a low-lying d-d state or states. Evidence for the d-d state has come from temperature-dependent lifetime^{5b-d} and photochemical ligand loss experiments.^{5d,8} In equivalent polypyridyl ligand environments, d-d states do not appear to play an important role for complexes of Os(II) compared to Ru(II). The major factor is no doubt that $10Dq$ is $\sim 30\%$ higher in the third transition series compared to the second⁹ so that low-lying d-d states occur at higher energies and are well removed from the emitting MLCT states.

We report here on the results of a solvent-dependence study on the lifetime and emission energies for the excited state(s) of $\text{Ru}(\text{bpy})_3^{2+}$, $\text{Ru}(\text{bpy})_3^{2+*}$. $\text{Ru}(\text{bpy})_3^{2+*}$ has been used as a sensitizer in a variety of media and it is important to establish and to attempt to rationalize the solvent dependence of its excited-state properties. For the case of $\text{Ru}(\text{bpy})_3^{2+}$, the problem is complicated by the presence of the low-lying d-d state(s) but, on the other hand, that complication offers an advantage. The advantage is that solvent effects can be explored both as to how they affect

(1) Kober, E. M.; Sullivan, B. P.; Dressick, W. J.; Caspar, J. V.; Meyer, T. J. *J. Am. Chem. Soc.* **1980**, *102*, 1383.

(2) Caspar, J. V.; Kober, E. M.; Sullivan, B. P.; Meyer, T. J. *J. Am. Chem. Soc.* **1982**, *104*, 630.

(3) Caspar, J. V.; Kober, E. M.; Sullivan, B. P.; Meyer, T. J. *Chem. Phys. Lett.* **1982**, *91*, 91.

(4) (a) Felix, F.; Ferguson, J.; Gudel, H. U.; Ludi, A. *J. Am. Chem. Soc.* **1980**, *102*, 4096. (b) Fujita, I.; Kobayashi, H. *Inorg. Chem.* **1973**, *12*, 2758. (c) Palmer, R. A.; Piper, T. S. *Ibid.* **1966**, *5*, 864.

(5) (a) Hager, G. D.; Crosby, G. A. *J. Am. Chem. Soc.* **1975**, *97*, 7031. (b) Allsopp, S. R.; Cox, A.; Kemp, T. J.; Reed, W. J. *J. Chem. Soc., Faraday Trans. 1* **1977**, 1275. (c) Van Houten, J.; Watts, R. J. *J. Am. Chem. Soc.* **1976**, *98*, 4853. (d) Durham, B.; Caspar, J. V.; Nagle, J. K.; Meyer, T. J. *Ibid.* **1982**, *104*, 4803. (e) Demas, J. N.; Taylor, D. G. *Inorg. Chem.* **1979**, *18*, 3177. (f) Gleria, M.; Minto, F.; Baggiato, G.; Bortolus, P. *J. Chem. Soc., Chem. Commun.* **1978**, 285.

(6) (a) Kober, E. M.; Meyer, T. J. *Inorg. Chem.* **1982**, *21*, 3978. Kober, E. M., Ph.D. Dissertation, University of North Carolina, 1982. (b) Hipps, K. W.; Crosby, G. A. *J. Am. Chem. Soc.* **1975**, *97*, 7042. (c) Hager, G. D.; Watts, R. J.; Crosby, G. A. *Ibid.* **1975**, *97*, 7037. (d) Ceulemans, A.; Vanquickenborne, L. G. *Ibid.* **1981**, *103*, 2238. (e) Daul, C. A.; Weber, J. *Chem. Phys. Lett.* **1981**, *77*, 593. (f) Belser, P.; Daul, C.; Von Zelewsky, A. *Ibid.* **1981**, *79*, 596.

(7) (a) Balzani, V.; Bolleta, F.; Gandolfi, M. T.; Maestri, M. *Top. Curr. Chem.* **1978**, *75*, 1. (b) Sutin, N.; Creutz, C. *Pure Appl. Chem.* **1980**, *52*, 2717. (c) Sutin, N. *J. Photochem.* **1979**, *10*, 19.

(8) (a) Hoggard, P. E.; Porter, G. B. *J. Am. Chem. Soc.* **1978**, *100*, 1457. (b) Wallace, W. M.; Hoggard, P. E. *Inorg. Chem.* **1980**, *19*, 2141. (c) Van Houten, J.; Watts, R. J. *Ibid.* **1978**, *17*, 3381.